Aalborg Universitet

Optimization Formulations for the Maximum Nonlinear Buckling Load of Composite Structures

Lindgaard, Esben; Lund, Erik

Optimization Formulations for the Maximum Nonlinear Buckling Load of Composite Structures

Esben Lindgaard · Erik Lund

Abstract This paper focuses on criterion functions for gradient based optimization of the buckling load of laminated composite structures considering different types of buckling behaviour. A local criterion is developed, and is, together with a range of local and global criterion functions from literature, benchmarked on a number of numerical examples of laminated composite structures for the maximization of the buckling load considering fiber angle design variables. The optimization formulations are based on either linear or geometrically nonlinear analysis and formulated as mathematical programming problems solved using gradient based techniques. The developed local criterion is formulated such it captures nonlinear effects upon loading and proves useful for both analysis purposes and as a criterion for use in nonlinear buckling optimization.

1 Introduction

Composite materials are mostly used in applications in aerospace and mechanical industries where their superior stiffness-to-weight or strength-to-weight ratios are critical. Designing structures made out of composite material represents a challenging task, since both thicknesses, number of plies in the laminate and their relative orientation must be selected. The best use of the capabilities of the material can only be gained through a careful selection of the layup. This may be achieved

Esben Lindgaard (✉) · Erik Lund
Department of Mechanical and Manufacturing Engineering,
Aalborg University, Aalborg, Denmark
Tel.: +45 99407329
Fax: +45 98151675
E-mail: elo@me.aau.dk

through a process of design optimization such that the material properties are tailored to meet particular structural requirements with little waste of material capability. A survey of optimal design of laminated plates and shells can be found in Abrate (1994). This work focuses on optimal design of laminated composite shell structures i.e. the optimal fiber orientations within the laminate which is a complicated problem. Laminated composite shell structures in service are commonly subjected to various kinds of compressive loads which may cause buckling. Hence, structural instability becomes a major concern in designing safe and reliable laminated composite shell structures.

In many works, e.g. Jones (2006), the buckling load is typically defined as the load at which the current equilibrium state of a structural element or structure suddenly changes from a stable to unstable configuration, and is, simultaneously, the load at which the equilibrium state suddenly changes from that previously stable configuration to another stable configuration. This may or may not be accompanied with large response, i.e. deformation or deflection. The buckling load is the largest load for which stability of equilibrium of a structural element or structure exists in its original equilibrium configuration. Considering simple/distinct stability points this definition of buckling only concerns the part classified as buckling with stability points in Fig. 1. The additional classification of simple stability points, given in Fig. 1, is well-known and printed in many textbooks, such as Thompson and Hunt (1973); Jones (2006). For limit point buckling, the buckling load is the load at the limit point and seen as a maximum point in a load-deflection diagram. In case of bifurcation buckling, the buckling load is the load at the bifurcation point where another equilibrium path, referred to as the secondary path, crosses the original/fundamental equilibrium path.

The role of imperfections, i.e. deviations from the perfect structure which in general can be geometrical, structural, material or load related, is illustrated in Fig. 1. A struc-
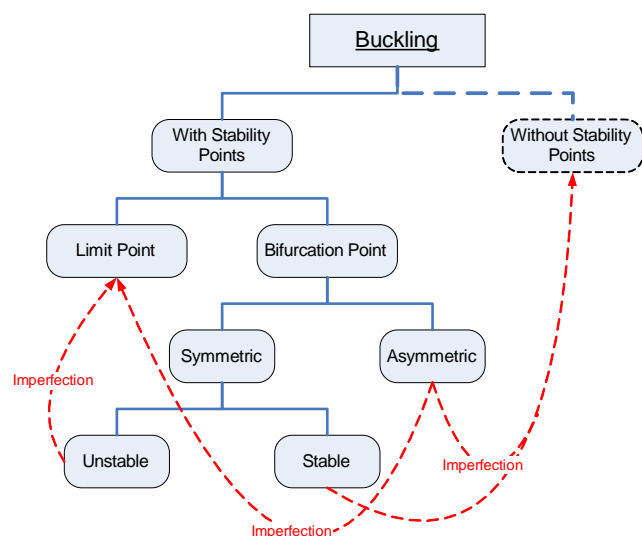
Fig. 1 Buckling classification considering simple stability points. Imperfections may change the type of buckling as marked by the red hatched lines.

ture that in its original perfect configuration is characterized by bifurcation buckling is with added imperfections either converted into a limit point instability or stable post buckling without having any stability point. Structural behaviour belonging to buckling without a stability point does in this study include imperfect structures with originally stable bifurcation a.k.a. stable post buckling, structures developing visual local buckling or wrinkles upon loading without bifurcation or limiting behaviour, and structures with geometrically nonlinear (GNL) behaviour with considerable geometry changes upon loading that acts in the same way as imperfections. The latter case is well-known and discussed e.g. by Brush and Almroth (1975); Bushnell (1985) in relation to buckling of compressed cylinders with cutouts. As discussed by Brush and Almroth (1975); Bushnell (1985) an initially straight cylinder with cutouts changes geometry upon compression and the structure bends near the cutouts such that a local buckling alike pattern starts to develop. Stiffness is lost in these regions as the local buckling alike pattern grows and the load is redistributed to other regions and the cylinder is able to carry far more loading before failure.

Considering the given definition of buckling these types of structural behaviour do certainly not fall within the category of buckling since no change in stability takes place. Such types of structural behaviour may be classified as pure structural nonlinear displacement mode evolutions upon loading. Nevertheless, the term buckling is often used in the characterization of these types of structural behaviour. This incoherency also exists in buckling experiments of plates where difficulties arise in determining a definite buckling load since the plates inherently are imperfect and therefore do not exhibit a stability point. In literature, several measures have been proposed in order to define a buckling load

of a structure that according to the above definition do not buckle. A collection of such measures to define a buckling load, in according to Jones (2006) a non-buckling event, for use in experimental studies are described in Singer et al (1998); Jones (2006).

To demonstrate that the above discussed structural behaviour not strictly may be classified as buckling the subcategory is connected loosely to buckling by a hatched line in Fig. 1. However the term buckling without stability point will be used in this paper to classify these types of structural behaviour.

Research on the subject of structural optimization of composite structures considering stability points has been reported by many investigators. In a finite element framework many authors, such as Lin and Yu (1991); Hyer and Lee (1991); Hu and Wang (1992); Walker et al (1996); Mateus et al (1997); Walker (2001); Foldager et al (2001); Hu and Yang (2007); Topal and Uzman (2008); Lund (2009); Topal (2009), have considered buckling optimization of composite structures where the buckling load was determined by the solution to the linearized discretized matrix eigenvalue problem at an initial prebuckling point, i.e. the linear buckling load. Moita et al (2000); Lindgaard and Lund (2010a); Lindgaard et al (2010) reported on nonlinear gradient based buckling optimization of composite laminated plates and shells where buckling is considered in terms of the limit load of the structure. Lindgaard and Lund (2010b) presented an optimization formulation that simultaneously handles bifurcation and limit point instability including geometrically nonlinear prebuckling effects.

Lee and Hinton (2000) studied linear strain energy minimization of shells with sizing and shape variables considering the improvement in nonlinear buckling limit load. They found for some examples an improvement in the nonlinear buckling load and for others a decrease and argued for the importance of accurately checking the stability limit of optimized shell structures by geometrically nonlinear analysis.

Overgaard and Lund (2005) applied local criterion functions, in terms of geometrically nonlinear determined principal element strains at a specified load level, in order to improve the buckling resistance of a laminated composite wind turbine blade.

Limited investigations have been devoted to buckling optimization of composite structures having buckling without stability points although this type of buckling often is encountered for real structures. Buckling without stability point may in some cases not be critical for the overall structural integrity since the load can be redistributed and the structure can continue to carry loading. For other structures, especially for laminated composite structures, local buckling and visual wrinkling may be crucial since it may govern the ultimate strength of the structure. Overgaard et al (2010) describes failure in a flapwise bending loaded wind

turbine blade, i.e. a large laminated composite structure, as a sequence of failure events where the first is delamination in the composite laminate triggered by local buckling and subsequently compressive fibre failure. It could also be postulated that a structure undergoing severe load redistribution due to the development of a local buckling pattern is unhealthy and operates in a manner, i.e. is carrying loading, that is not intended by the design engineer. Thus, there is a lack of optimization formulations that is able to deal with buckling without stability points. Furthermore, it is unclear how well the different existing optimization criteria perform compared to one another and to the type of buckling.

This paper deals with the above mentioned problems and benchmarks a number of objective functions in the attempt to maximize the buckling resistance on a range of different numerical examples of laminated composite structures characterized by different types of buckling. Buckling with stability point of the limit point type and buckling without stability point is considered. The already mentioned global and local buckling criteria from literature are applied in the benchmark study and a new local criterion is developed and presented. Linear and geometrically nonlinear analysis is applied for the different criteria in order to investigate the importance of including geometrically nonlinear prebuckling effects. The developed local criterion is based on geometrically nonlinear analysis and formulated such it detects and captures local nonlinear effects upon loading. It is referred to as the nonlinearity factor criterion. Design sensitivities of all buckling criterion functions are obtained semi-analytically by either the direct differentiation approach or by the adjoint approach and the optimization problems are set up as mathematical programming problems solved by a gradient based optimization algorithm.

In this work only Continuous Fiber Angle Optimization (CFAO) is considered, thus fiber orientations in laminate layers with preselected thickness and material are chosen as design variables in the laminate optimization. Although fiber angle optimization is known to be associated with a non-convex design space with many local minima it has been applied since the laminate parametrization has not been the focus in this work, i.e. the presented methods in this paper are generic and can easily be used with other parametrizations.

The governing equations for linear and nonlinear buckling analysis are presented in Sect. 2 together with features applied for buckling detection during geometrically nonlinear analysis. The different buckling objective functions applied in the benchmark study are presented in Sect. 3 and the optimization formulations are stated in Sect. 4. The benchmark study of the different buckling objective functions are conducted upon a series of numerical examples of laminated composite structures in Sections 5, 6, and 7. Conclusions are outlined in Sect. 8.

2 Buckling analysis and detection

The finite element method is used for determining the buckling load of the laminated composite structure, thus the derivations are given in a finite element context.

A laminated composite is typically composed of multiple materials and multiple layers, and the shell structures can in general be curved or doubly-curved. The materials used in this work are fiber reinforced polymers, e.g. Glass or Carbon Fiber Reinforced Polymers (GFRP/CFRP), oriented at a given angle θ_k for the kth layer. All materials are assumed to behave linearly elastic and the structural behaviour of the laminate is described using an equivalent single layer theory where the layers are assumed to be perfectly bonded together such that displacements and strains will be continuous across the thickness.

The solid shell elements used are derived using a continuum mechanics approach so the laminate is modelled with a geometric thickness in three dimensions, see Johansen et al (2009). The element used is an eight node isoparametric element where shear locking and trapezoidal locking is avoided by using the concepts of assumed natural strains for respectively out of plane shear interpolation, see Dvorkin and Bathe (1984), and through the thickness interpolation, see Harnau and Schweizerhof (2002). Membrane and thickness locking is avoided by using the concepts of enhanced assumed strain for the interpolation of the membrane and thickness strains respectively, see Klinkel et al (1999).

2.1 Linear buckling analysis

Linear buckling analysis is a classical engineering method for determining the buckling load of structures. The method gives numerical inexpensive predictions of buckling with stability point, i.e. singular tangent stiffness. For shell structures it is often used as a generalized stability predictor, as described in Almroth and Brogan (1972), when the stability point is of bifurcation or even limit point type. Linear buckling analysis is based upon linear static analysis where the static equilibrium equation for the structure may be written as

$$\mathbf{K}_0 \mathbf{D} = \mathbf{R} \tag{1}$$

Here $\mathbf{D}$ is the global displacement vector, $\mathbf{K}_0$ is the global initial stiffness matrix, and $\mathbf{R}$ the global load vector.

Based on the displacement field, obtained by the solution to (1), the element layer stresses can be computed, whereby the stress stiffening effects due to mechanical loading can be evaluated by computing the initial stress stiffness matrix $\mathbf{K}_\sigma$. By assuming the structure to be perfect with no geometric imperfections, stresses are proportional to the loads, i.e. stress stiffness depends linearly on the load, displacements

at the critical/buckling configuration are small, and the load is independent of the displacements, the linear buckling problem can be established as

$$(\mathbf{K}_0 + \lambda_j \mathbf{K}_\sigma)\, \phi_j = \mathbf{0}, \qquad j = 1, 2, \ldots, J \qquad (2)$$

where the eigenvalues are ordered by magnitude, such that λ_1 is the lowest eigenvalue, i.e. buckling load factor, and ϕ_1 is the corresponding eigenvector i.e. buckling mode. In general, for engineering shell structures, the eigenvalue problem in (2) can be difficult to solve, due to the size of the matrices involved and large gaps between the distinct eigenvalues. For efficient and robust solutions, (2) is solved by a subspace method with automatic shifting strategy, Gram-Schmidt orthogonalization, and the sub-problem is solved by the Jacobi iterations method, see Wilson and Itoh (1983).

2.2 Nonlinear buckling analysis

Better predictions of structural buckling with stability points than that available by linear buckling analysis may be achieved by nonlinear buckling analysis. The method incorporates geometrically nonlinear analyses and applies for both bifurcation and limit point instability, depending on what to appear on the equilibrium path.

Let us consider geometrically nonlinear behaviour of structures made of linear elastic materials. We adopt the Total Lagrangian approach, i.e. displacements refer to the initial configuration, for the description of geometric nonlinearity. An incremental formulation is more suitable for nonlinear problems and it is assumed that the equilibrium at load step n is known and it is desired at load step $n + 1$. Furthermore, it is assumed that the current load is independent on deformation. The incremental equilibrium equation in the Total Lagrangian formulation is written as (see e.g. Brendel and Ramm (1980); Hinton (1992))

$$\mathbf{K_T}(\mathbf{D}^n, \gamma^n)\, \delta \mathbf{D} = \mathbf{R}^{n+1} - \mathbf{F}^n \qquad (3)$$
$$\mathbf{K_T}(\mathbf{D}^n, \gamma^n) = \mathbf{K_0} + \mathbf{K_L}(\mathbf{D}^n, \gamma^n) + \mathbf{K}_{\boldsymbol{\sigma}}(\mathbf{D}^n, \gamma^n) \qquad (4)$$
$$\mathbf{K_T}^n = \mathbf{K_0} + \mathbf{K_L}^n + \mathbf{K}_{\boldsymbol{\sigma}}^n \qquad (5)$$

Here $\delta \mathbf{D}$ is the incremental global displacement vector, $\mathbf{F}^n$ global internal force vector, and $\mathbf{R}^{n+1}$ global applied load vector. The global tangent stiffness $\mathbf{K_T}^n$ consists of the global initial stiffness $\mathbf{K_0}$, the global stress stiffness $\mathbf{K}_{\boldsymbol{\sigma}}^n$, and the global displacement stiffness $\mathbf{K_L}^n$. The applied load vector $\mathbf{R}^n$ is controlled by the stage control parameter (load factor) γ^n according to an applied reference load vector $\mathbf{R}$

$$\mathbf{R}^n = \gamma^n \mathbf{R} \qquad (6)$$

The incremental equilibrium equation (3) is solved by the arc-length method after Crisfield (1981).

During the nonlinear path tracing analysis we can at some converged load step estimate an upcoming critical point, i.e. bifurcation or limit point, by utilizing tangent information. At a critical point the tangent operator is singular

$$\mathbf{K_T}(\mathbf{D}^c, \gamma^c)\phi_j = \mathbf{0} \qquad (7)$$

where the superscript c denotes the critical point and ϕ_j the buckling mode. To avoid a direct singularity check of the tangent stiffness, it is easier to utilize tangent information at some converged load step n and extrapolate it to the critical point. The one-point approach only utilizes information at the current step and extrapolates by only one point, see Brendel and Ramm (1980); Borri and Hufendiek (1985). The stress stiffness part of the tangent stiffness at the critical point is approximated by extrapolating the nonlinear stress stiffness from the current configuration as a linear function of the load factor γ.

$$\mathbf{K}_{\boldsymbol{\sigma}}(\mathbf{D}^c, \gamma^c) \approx \lambda \mathbf{K}_{\boldsymbol{\sigma}}(\mathbf{D}^n, \gamma^n) = \lambda \mathbf{K}_{\boldsymbol{\sigma}}^n \qquad (8)$$

It is assumed that the part of the tangent stiffness consisting of $\mathbf{K_L}^n$ and $\mathbf{K_0}$ does not change with additional loading, which holds if the additional displacements are small. The tangent stiffness at the critical point is approximated as

$$\mathbf{K_T}(\mathbf{D}^c, \gamma^c) \approx \mathbf{K_0} + \mathbf{K_L}^n + \lambda \mathbf{K}_{\boldsymbol{\sigma}}^n \qquad (9)$$

and by inserting into (7) we obtain a generalized eigenvalue problem

$$(\mathbf{K_0} + \mathbf{K_L}^n)\, \phi_j = -\lambda_j \mathbf{K}_{\boldsymbol{\sigma}}^n \phi_j \qquad (10)$$

where the eigenvalues are assumed ordered by magnitude such that λ_1 is the lowest eigenvalue and ϕ_1 the corresponding eigenvector. The solution to (10) yields the estimate for the critical load factor at load step n as

$$\gamma_j^c = \lambda_j \gamma^n \qquad (11)$$

If $\lambda_1 < 1$ the first critical point has been passed and in contrary $\lambda_1 > 1$ the critical point is upcoming. The one-point procedure works well for both bifurcation and limit points. The closer the current load step gets to the critical point, the better the approximation becomes, and it converges to the exact result in the limit of the critical load.

2.3 Buckling detection in GNL analysis

Several different stop criteria are applied for the GNL analyses from which an equilibrium point is determined for the design sensitivity analysis (DSA) during the optimization, see Table 1. In the case of buckling with a stability point in the form of a limit point, a limit point detector criterion may be used. The limit load is simply detected by monitoring the load factor in the GNL analysis, see (3). When the load factor from two successive load steps decreases the

previous converged load is defined as the limit load. A bifurcation point detector, as described in Lindgaard and Lund (2010b), may be applied in case of bifurcation buckling. For bifurcation point detection nonlinear buckling analysis is performed at precritical stages during GNL analysis as a singularity check on the tangent stiffness. Since buckling of structures due to bifurcation is not concerned in the present paper this has not been further addressed.

Table 1 Stop criteria applied for buckling detection in GNL analysis.

With stability point
Limit point detection
Bifurcation point detection
Without stability point
At load level
At maximum displacement
At maximum nonlinearity factor, ε_{GNL}

In the case of buckling without any stability point other stop criteria for the GNL analysis are needed. The GNL analysis may be proceeded towards a certain load level. Even though buckling is not detected by this stop criterion it is applied in the study to investigate the effect of having the chosen equilibrium point for the DSA located closely or far away from the buckling point. A simple maximum displacement criterion monitoring the maximum displacement during GNL analysis is also applied as a stop criterion for the GNL analysis. Since buckling of a structure typically causes the displacements to increase disproportionate in comparison to the load this criterion may be able to detect buckling. At last a so-called nonlinearity factor criterion, ε_{GNL}, is developed and applied in the study, see (12). The criterion is formulated such it detects local nonlinear effects in the structural behaviour during loading. Buckling of structures are in many cases associated with nonlinear effects and extensive load redistribution which has been the motivation for the developed criterion. The criterion is based on the fraction between the principal element strain and the load factor. The relative change in the fraction from the initial load step 1 to the current load step n defines the element nonlinearity factor.

$$\varepsilon_{\text{GNL}} = 1 + \left| \frac{\varepsilon_1^n/\gamma^n - \varepsilon_1^1/\gamma^1}{\varepsilon_1^1/\gamma^1} \right| \tag{12}$$

The nonlinearity factor for linear behaviour is $\varepsilon_{\text{GNL}} = 1.0$ and larger than one when nonlinear behaviour occurs. The stop criterion based on the nonlinearity factor may be activated for all elements in the numerical model or only elements belonging to certain parts of the structure. Note that all stop criteria described for buckling without stability points, see Table 1, also may be applied in the case of buckling with stability point.

3 Buckling objective functions

A range of different objective functions are investigated and considered for the maximum buckling resistance. The objective functions are described in the following and comments about the design sensitivity analysis of the different objective functions are given. The equations for the design sensitivity analysis are stated in Appendix A.

For the design sensitivities of all objective functions involving geometrically nonlinear analyses it is assumed that the applied loads are independent of design changes and displacements. This is true in the case of laminate optimization with fiber angle design variables and with conservative loading, i.e. no follower loads. Furthermore, it is assumed that the end load level for the design sensitivity analysis is fixed. The latter is not always true since the final load level in some GNL analyses are determined by a GNL stop criterion which is not based on a constant load level, see Table 1. If constant load level is not assumed very complicated and numerical costly design sensitivity analysis has to be invoked, see Noguchi and Hisada (1993). Applying the fixed load assumption the design sensitivity analysis becomes more simple and numerical efficient since the sensitivities can be obtained solely by information at the final equilibrium point. If the optimization procedures applying this assumption converge towards a constant load level the assumption becomes valid.

3.1 Linear compliance

Linear compliance C_L is defined as the work done by the applied loads at the equilibrium state expressed in terms of the linear static equilibrium equation stated in (1).

$$C_L(\mathbf{D}) = \mathbf{R}^{\text{T}} \mathbf{D} \tag{13}$$

3.2 Nonlinear end compliance

Nonlinear end compliance C_{GNL} is defined as the work done by the applied loads at the equilibrium state at the final load step n expressed in terms of the nonlinear incremental equilibrium equation stated in (3).

$$C_{GNL}(\mathbf{D}^n, \mathbf{R}^n) = (\mathbf{R}^n)^{\text{T}} \mathbf{D}^n \tag{14}$$

The expression for the nonlinear end compliance in (14) is in general dependent on both the displacements, $\mathbf{D}^n$ and the external load, $\mathbf{R}^n$ at the final load step n. Considering design changes the nonlinear end compliance criterion applied in this study is only considered dependent upon the displacements $\mathbf{D}^n$ at the chosen load step n whereas the applied load $\mathbf{R}^n$ is considered independent upon design changes, i.e. $C_{GNL}(\mathbf{D}^n(\mathbf{a}), \mathbf{R}^n)$ where the design variables $a_i, i = 1, \ldots, I$, are collected in $\mathbf{a}$.

3.3 Nonlinear first principal element strain

An objective function based on the first nonlinear principal element strain, ε_1, is applied in the study since local buckling of structures typically is related to large increase in displacements of certain parts of the structure which eventually may result in high strains. Thus, minimizing the element strains may prove to be a way of improving the buckling resistance of a structure. For every converged load step n in (3) the element strain tensor may be calculated on basis of the displacement field from which the principal element strains can be expressed.

3.4 Element nonlinearity factor

The element nonlinearity factor, $\varepsilon_{\mathrm{GNL}}$, defined by (12) between an initial load step and the current load step is also implemented as objective function in the study. As explained earlier, buckling of structures is in many cases associated with nonlinear effects and extensive load redistribution. The element nonlinearity factor is a local criterion that is developed such it detects nonlinear effects during loading, thus minimizing the element nonlinearity factor may improve the buckling resistance of a structure.

3.5 Linear buckling

The linear buckling load is obtained as the lowest eigenvalue of (2). Traditionally, the linear buckling load is considered as objective when the task is to improve the buckling resistance of structures and therefore applied in the study as a frame of reference.

3.6 Nonlinear buckling

The nonlinear buckling load is determined at a precritical load level using the one-point approach by solving the eigenvalue problem in (10) and estimating the buckling load by linear extrapolation in (11). Better predictions of the buckling load are generally obtained by nonlinear buckling analysis compared to the traditional linear buckling analysis. Conversely is nonlinear buckling analysis more complicated and numerical expensive than linear buckling analysis since it requires geometrically nonlinear analysis to trace the equilibrium path. The nonlinear buckling load is formulated as an objective function by the procedures originally proposed in Lindgaard and Lund (2010a); Lindgaard et al (2010). The expressions for the design sensitivities are as for the other objective functions described in Appendix A.

4 Optimization formulations

A range of different optimization formulations is applied in the study in the attempt to improve the buckling resistance of a composite structure. The design variables in the numerical studies are fiber angles in the laminate layup of a laminated composite structure. The optimization problems are all formulated as either a max-min problem or a min-max problem. The direct formulation of the optimization problem can give problems related to differentiability and fluctuations during the optimization process since, e.g. the eigenvalues in the linear buckling problem may change position, i.e. the second lowest eigenvalue can become the lowest. An elegant solution to this problem is to make use of the so-called bound formulation, see Bendsøe et al (1983); Taylor and Bendsøe (1984); Olhoff (1989). A new artificial variable β is introduced and a new artificial objective function β is chosen. An equivalent problem is formulated, where the previous non-differentiable objective function is transformed into a set of constraints. Considering a general multi objective function F_j containing N_F function values, the mathematical programming problem may be formulated as

$$\text{Objective}: \max_{\boldsymbol{a}, \beta} \ \beta \ \text{ or } \ \min_{\boldsymbol{a}, \beta} \ \beta$$

$$\text{Subject to}: F_j \geq \beta \ \text{ or } \ F_j \leq \beta, \quad j = 1, \ldots, N_F$$
$$\underline{a_i} \leq a_i \leq \overline{a_i}, \quad i = 1, \ldots, I$$

where a_i denote the laminate design variables in terms of fiber angles. In case of an objective with many local criterion functions, such as min-max nonlinear first principal element strain, an active set strategy is employed in order to reduce the number of local criterion functions. Only criterion functions with a value larger than 70% of the maximum criteria function are included in the active set. The mathematical programming problems are solved by the Method of Moving Asymptotes (MMA) by Svanberg (1987). The closed loop of analysis, design sensitivity analysis and optimization is repeated until convergence in the design variables or until the maximum number of allowable iterations has been reached.
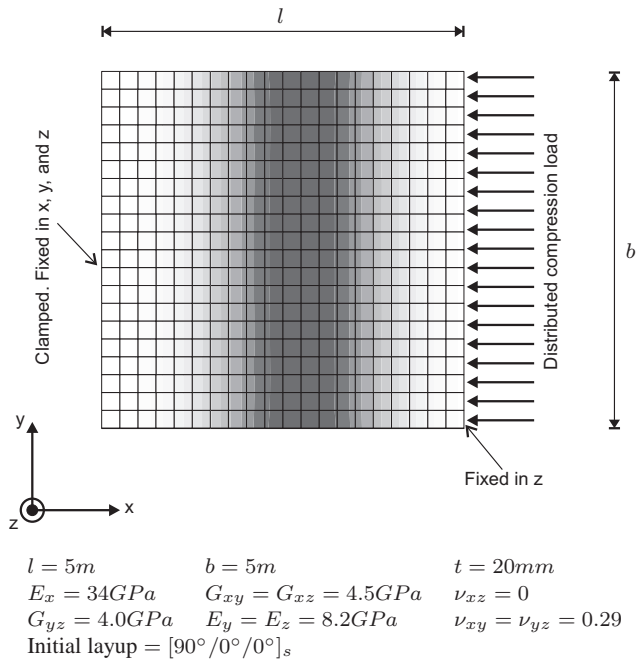
The numerical efficiency of the different optimization formulations depends on the analysis method and the design sensitivity analysis utilized. Please refer to Appendix A for details about the design sensitivity analysis. Obviously, linear analysis is more attractive than geometrically nonlinear analysis in terms of computational cost. The design sensitivity analyses of the linear and nonlinear buckling load are comparable in computational cost but are the most numerical demanding of all objective functions considered. The computational cost of the design sensitivity analysis of the element nonlinearity factor and the nonlinear first principal element strain are less than the linear and nonlinear buck-

ling load but higher than the linear and nonlinear compliance since the displacement sensitivities need to be computed.

5 Numerical example: laminated composite imperfect plate

The clamped composite laminated plate subjected to a distributed compression load, see Fig. 2, is a structure that has a stable symmetric point of bifurcation. The bifurcation load for the perfect plate estimated by a linear buckling analysis is $438kPa$. According to Fig. 1 introductions of imperfections remove the stability point and changes the structural response to a single stable equilibrium path without a stability point.

$$l = 5m \qquad b = 5m \qquad t = 20mm$$
$$E_x = 34GPa \qquad G_{xy} = G_{xz} = 4.5GPa \qquad \nu_{xz} = 0$$
$$G_{yz} = 4.0GPa \qquad E_y = E_z = 8.2GPa \qquad \nu_{xy} = \nu_{yz} = 0.29$$
Initial layup = $[90°/0°/0°]_s$

Fig. 2 Geometry, loads, boundary conditions, and material properties for the laminated composite plate example. The total thickness of the plate is denoted by t and the layup has an equal ply thickness. The fundamental buckling mode is also shown in contours on the plate. The plate is modelled by 400 equivalent single layer solid shell finite elements.

This characteristic is utilized to construct a simple example for which buckling appears without any stability points. Geometric imperfections according to the first linear buckling mode, see Fig. 2, is superimposed upon the geometry with a specified amplitude. The amplitude is defined as the largest translational component of the first linear buckling mode relative to the thickness of the plate. For this example an imperfection amplitude of 1% has been applied to generate an example that buckles without a stability point. Since buckling for the imperfect plate appears without any stability point the buckling load has to be manually determined

by visual inspection of the equilibrium curve. The equilibrium path for the initial imperfect plate is shown in Fig. 3. The buckling load is defined when the displacement starts to grow rapidly, i.e. the equilibrium path changes direction from the initial part of the path.

A range of different optimization formulations for the maximum buckling resistance is benchmarked upon the example. The fiber angle in all six fiber layers are used as design variables. An optimization formulation involving nonlinear buckling analysis cannot be used since buckling appears without a stability point. Linear buckling optimization is applied as a frame of reference although no stability point is present. The optimization formulations benchmarked upon the imperfect composite laminated plate example are stated in Table 2.

Nine different optimization approaches are applied in the buckling optimization of the imperfect laminated composite plate. Optimization formulation number one and two, see Table 2, applies linear analysis while the others utilize geometric nonlinear analysis. For the optimizations with geometric nonlinear analysis three different stop criteria have been applied to terminate the geometric nonlinear analysis. For e.g. the compliance minimizations, optimization formulation number three always complete the GNL analysis to the same load level, namely a load of $550kPa$ which is slightly above the buckling load of the initial design. For optimization formulation four and five the GNL analysis is performed towards different load levels at each optimization iteration and controlled by a maximum displacement and a maximum nonlinearity factor criterion $\varepsilon_{\mathrm{GNL}}$, respectively. The threshold values for these stop criteria are set such that the reached load level in the GNL analysis is close to the buckling load. The threshold value for the maximum displacement u in x-direction is set to $7mm$ and the maximum nonlinearity factor is set to $\varepsilon_{\mathrm{GNL}} = 20$. Optimization formulation number six and seven minimize the maximum first principal strains, ε_1, whereas optimization formulation eight and nine minimize the maximum nonlinearity factor, $\varepsilon_{\mathrm{GNL}}$.

The equilibrium curves of the optimized designs according to the approaches stated in Table 2 are shown in Fig. 3. Almost all optimization approaches lead towards designs with nearly the same equilibrium path and only minor differences are traceable in the buckling load improvements shown in Fig. 4.

The laminate designs for all optimization approaches are driven towards zero degrees fiber angles in all design layers. However for optimization approach four, six, and eight the fiber angle in design layer four for the optimized designs is around $60°$ and for optimization approach nine the fiber angle in design layer three and four are $-89°$ and $104°$, respectively.

**Table 2** Optimization formulations applied in the buckling optimization of the imperfect laminated composite plate.

#	Objective function	Analysis method	Stop criterion
1.	Max Min Linear Buckling	Linear	-
2.	Min Linear Compliance	Linear	-
3.	Min Compliance	GNL	Load
4.	Min Compliance	GNL	Disp.
5.	Min Compliance	GNL	ε_{GNL}
6.	Min Max ε_1	GNL	Disp.
7.	Min Max ε_1	GNL	ε_{GNL}
8.	Min Max ε_{GNL}	GNL	Disp.
9.	Min Max ε_{GNL}	GNL	ε_{GNL}
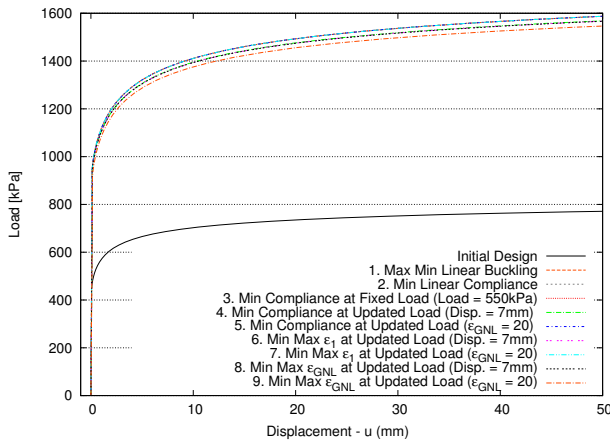
Fig. 3 Load-deflection curves of the initial laminate composite design and of the optimized designs obtained by the benchmarked optimization formulations. The displacement is measured at mid span on the loaded side of the plate and positive in the loading direction.
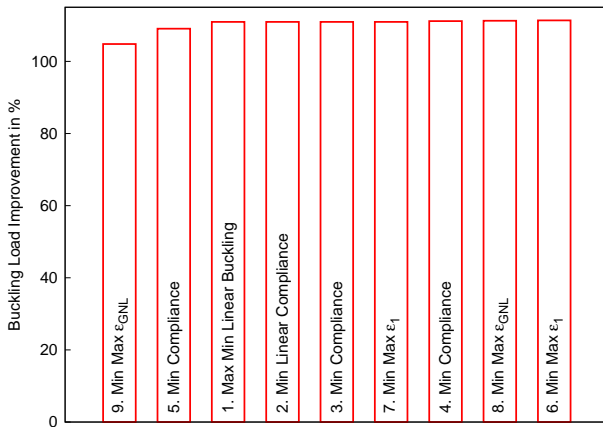
Fig. 4 Buckling load improvement in percent of the imperfect laminated composite plate for the benchmarked optimization formulations.

All the benchmarked optimization formulations give satisfactory results and are nearly equally good in increasing the buckling resistance for the imperfect laminated composite plate.

6 Numerical example: laminated composite U-profile

The laminated composite U-profile is an example of a real structural engineering element. Geometry, loading, and boundary conditions are identical to a model analyzed by Klinkel et al (1999); Lindgaard and Lund (2010a); Lindgaard et al (2010). The U-profile is clamped at one end and point loaded in an upper corner node at the other end with a force $R = 250 kN$. A total of 432 equivalent single layer solid shell finite elements is used in the numerical model.
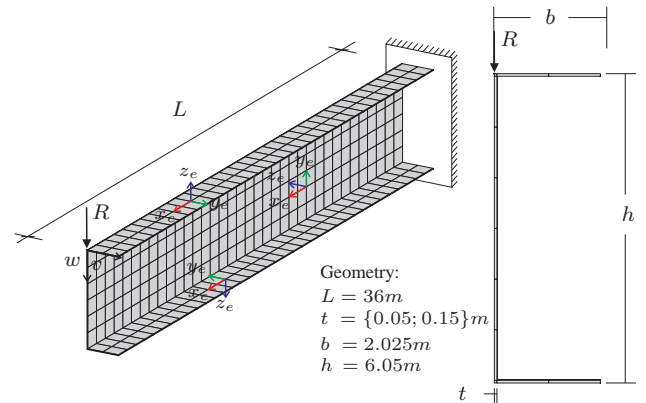
Fig. 5 Geometry, loads, boundary conditions, and element coordinate systems for numerical model of the U-profile.

Two thickness configurations of the U-profile are considered, i.e. $t = \{0.05; 0.15\} m$. This leads to two different types of buckling behaviour. The first configuration which defines case 1 buckles due to a limit point instability whereas case 2 buckles without any stability point, see e.g. Fig. 1. The laminate layup consists of 4 uni-directional E-glass/epoxy fiber layers each of equal thickness, see properties of the processed material in Table 3.

The fiber orientation is related to the element coordinate system, (x_e, y_e, z_e), in each finite element. The fiber orientation is measured counterclockwise from the x-axis in the xy-plane of the element coordinate system. The element coordinate system for the finite elements in the web and each flange, respectively, is depicted in Fig. 5. The fiber orienta-

8

Table 3 Processed material properties for U-profile.

E-glass/epoxy			
E_x	30.6 GPa	E_y	8.7 GPa
E_z	8.7 GPa	ν_{xy}	0.29
ν_{xz}	0.3	ν_{yz}	0.3
G_{xy}	3.24 GPa	G_{xz}	3.24 GPa
G_{yz}	2.9 GPa	ρ	1686 kg/m^3

tion of each layer for the web and each flange, respectively, is considered constant and the layer stacking is done from inside out. The initial layup definition for the U-profile is stated in Table 4.

Table 4 Layup definition for the U-profile. Each layer in the laminate layup has equal thickness.

Layup definition	
Top Flange	$(0°, 45°, −90°, −45°)$
Web	$(90°, 135°, 0°, 45°)$
Bottom Flange	$(45°, 90°, −45°, 0°)$

The fiber angles in the layup definition are used as laminate design variables in the benchmark study of the different optimization formulations for maximum buckling resistance. Since the U-profile consists of 4 uni-directional fiber layers at web and each flange this yields a total of 12 design variables.

6.1 U-profile case 1

Initial analysis of the U-profile with a thickness of $t = 0.05m$ shows buckling of the structure due to a limit point instability. The linear buckling load and the equilibrium curve from a geometrically nonlinear analysis are depicted in Fig. 6. Linear buckling analysis is unable to predict the limit point instability and overestimates the buckling load by 27%.

The geometrically nonlinear analysis predicts buckling due to a limit point instability where the structure buckles in the top flange near the fixed support, see Fig. 7. In contrary, linear buckling analysis predicts bifurcation buckling due to collapse in the web section at the free end.

The optimization formulations stated in Table 5 are benchmarked upon the U-profile with a thickness of $t = 0.05$. Since the structure buckles due to a limit point stability, a stability point is present, thus optimization formulations based on linear and nonlinear buckling analysis may be applied. Note that the numbering of the optimization formulations for this numerical example, see Table 5, is different from that of the previous example, see Table 2.

For the optimization formulations involving geometrically nonlinear analysis three different stop criteria have been applied to terminate the geometrically nonlinear analysis.
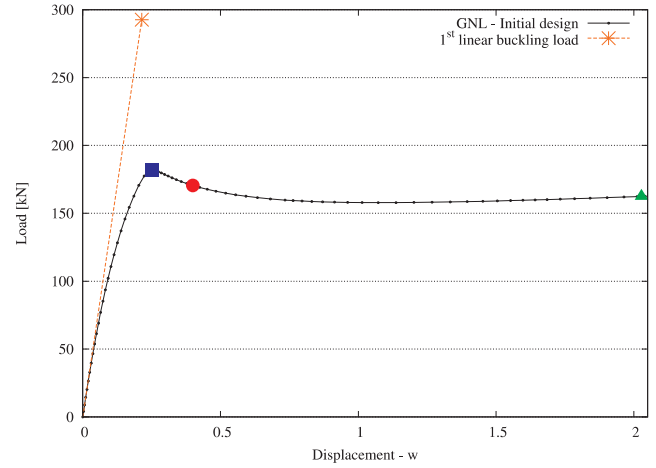
Fig. 6 Linear buckling load and load displacement curve from geometrically nonlinear analysis of U-profile.
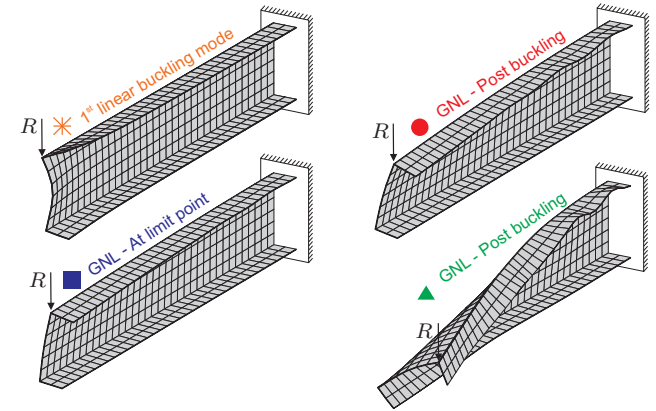
Fig. 7 1st linear buckling mode shape and displacement field at different load steps during the geometrically nonlinear analysis. Note that the displacement fields correspond to the marked equilibrium points on the load displacement curve in Fig. 6.

Those with load based stop criterion continue the GNL analysis until a certain load level is reached. A load of $125kN$ is used in the load based stop criterion. For the optimization formulations with a stop criterion for the GNL analysis based on either a limit point detector or a maximum nonlinearity factor ε_{GNL}, the GNL analysis may be terminated at different load levels for each optimization iteration. The maximum nonlinearity factor is set to 15 in the stop criterion which for the initial laminate design is reached at a load of $166kN$.

Load-deflection curves of the optimized designs are collected in Fig. 8 and the buckling load improvement by the benchmarked formulations are shown in Fig. 9. All the optimized designs maintain the same buckling type, i.e. limit point instability, and all optimization formulations manage to improve the buckling load.

The poorest performing optimization formulations are those based on linear analysis, i.e. optimization formulation one and three. The best performing optimization formulation is number two which is based on the nonlinear

9

Table 5 Optimization formulations applied in the buckling optimization of the U-profile case 1.

#	Objective function	Analysis method	Stop criterion
1.	Max Min Linear Buckling	Linear	-
2.	Max Min Nonlinear Buckling	GNL	Limit Point
3.	Min Linear Compliance	Linear	-
4.	Min Compliance	GNL	Load
5.	Min Compliance	GNL	Limit Point
6.	Min Max ε_1	GNL	Limit Point
7.	Min Max ε_{GNL}	GNL	Load
8.	Min Max ε_{GNL}	GNL	Limit Point
9.	Min Max ε_{GNL}	GNL	ε_{GNL}
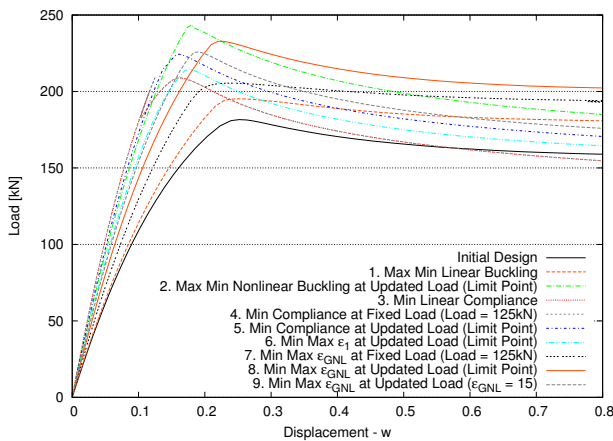
Fig. 8 Load-deflection curves of the initial laminate composite design and of the optimized designs obtained by the benchmarked optimization formulations.
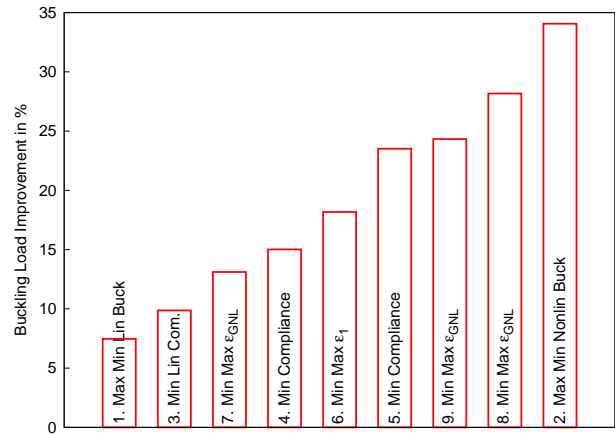
Fig. 9 Buckling load improvement in percent of the U-profile case 1 by the benchmarked optimization formulations.

buckling load. Among the optimization formulations based on the minimization of the maximum nonlinearity factor those stopped close to the stability point yield the best performance. This observation also holds for the optimization formulations based on geometrically nonlinear compliance minimization. This means that the performance of optimization formulations having same objective function can be ranked according to the stop criterion applied in the GNL analysis, i.e. limit point, ε_{GNL}, and load.

6.2 U-profile case 2

The U-profile is again considered with same properties as in case 1 except the thickness which is changed to $t = 0.15m$. With this configuration the structure buckles without a stability point, i.e. the equilibrium path keeps rising stably without any bifurcation or limit point. The equilibrium path for the initial laminate design is shown in Fig. 11. The U-profile buckles visually in the top flange near the fixed support as in case 1, see Fig. 10. The equilibrium point the buckle starts to develop is marked on the equilibrium path in Fig. 11.
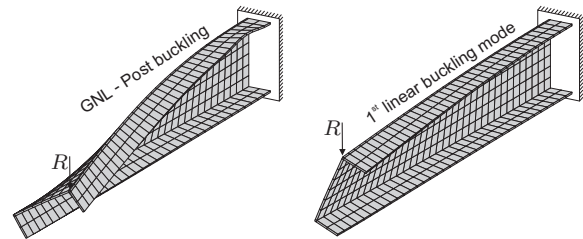
Fig. 10 1st linear buckling mode shape and post buckling displacement field for the initial design of the U-profile case 2.
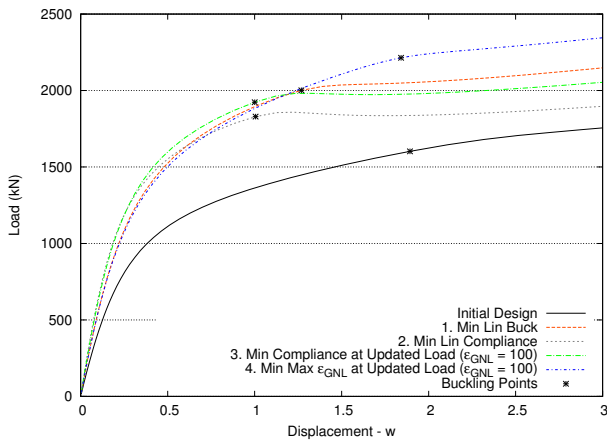
The benchmarked optimization formulations are stated in Table 6. Although no stability point is present for the example the optimization formulation based on the linear buckling load is attempted. The fundamental linear buckling mode for case 2 is differently from that determined in case 1. The fundamental linear buckling mode for the initial design of U-profile case 2 is shown in Fig. 10. The linear buckling mode is very similar to the geometrically nonlinear deformation shape and is best described as a flexural-torsional buckling mode.

For optimization formulation number three and four a stop criterion based on the maximum nonlinearity factor is applied to terminate the GNL analysis. The maximum non-

linearity factor is set to 100 which for the initial design is reached at a load of $1600kN$.

The equilibrium curves of the optimized designs obtained by the benchmarked optimization formulations are collectively shown in Fig. 11. The load level at which a buckle starts to develop in the top flange is marked on the equilibrium curves and is purely determined by visual inspection of the deformation shape. Considering this point as the buckling load, the best improvement is obtained by optimization formulation number four that minimizes the maximum nonlinearity factor in the structure. Surprisingly, the second best design is obtained by optimization formulation number one that maximizes the linear buckling load, despite the absence of a stability point.


Fig. 11 Load-deflection curves of the initial laminate composite design and of the optimized designs obtained by the benchmarked optimization formulations for U-profile case 2.

Using the optimization formulations based on minimum compliance, i.e. optimization formulation two and three, a stability point in the form of a limit point is introduced during optimization. The compliance minimization based on GNL analysis performs better than the linear compliance optimized design which again demonstrates the importance of including nonlinear prebuckling displacements.

7 Numerical example: laminated composite box-profile

The laminated composite box-profile depicted in Fig. 12 is clamped at one end and point loaded at the other end. The box-profile is divided into five structural parts which consist of two webs and three flanges. A total of 1980 equivalent single layer solid shell finite elements is used in the numerical model.

The laminate layup consists of 4 uni-directional E-glass/epoxy fiber layers, each of equal thickness, for each of the five
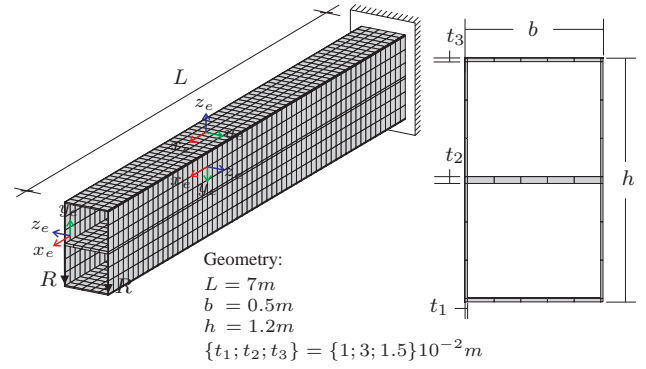
Fig. 12 Geometry, loads, boundary conditions, and element coordinate systems for the numerical model of the box-profile.

structural parts in the box-profile, see Table 7. The material properties of the uni-directional E-glass/epoxy are identical to those used for the U-profile example, see Table 3. The fiber orientation is again related to the element coordinate system, (x_e, y_e, z_e), in each finite element and the same orientational definition of the fiber layers as used for the U-profile is applied. The element coordinate system for the finite elements for the webs and flanges are shown in Fig. 12. The fiber orientation of each layer for each of the five structural parts is considered constant throughout the length of the profile and the layer stacking is done in accordance with the z_e-axis. The fiber angles in the layup definition are used as laminate design variables in the benchmark study of the optimization formulations which gives a total of 20 design variables.

Initial analyses of the box-profile show that the structure buckles without any loss of stability and without any points of stability, i.e. limit point or bifurcation point. The load-deflection curve of the initial design obtained by a geometrically nonlinear analysis is depicted in Fig. 15 and deformation shapes at different load levels are shown in Fig. 13 together with the first linear buckling mode.
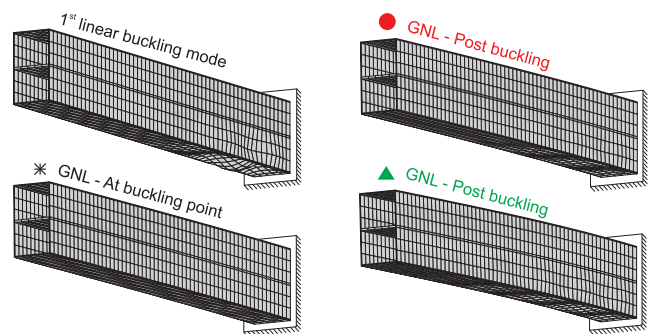
Fig. 13 1st linear buckling mode shape and displacement field at different load steps during the geometrically nonlinear analysis. Note that the displacement fields correspond to the marked equilibrium points (80, 127, and $195kN$) on the load displacement curve in Fig. 15 for the initial design.

Table 6 Optimization formulations applied in the buckling optimization of the U-profile case 2.

#	Objective function	Analysis method	Stop criterion
1.	Max Min Linear Buckling	Linear	-
2.	Min Linear Compliance	Linear	-
3.	Min Compliance	GNL	$\varepsilon_{\mathrm{GNL}}$
4.	Min Max $\varepsilon_{\mathrm{GNL}}$	GNL	$\varepsilon_{\mathrm{GNL}}$

Table 7 Layup definition for the box-profile. Each layer in the laminate layup has equal thickness.

Layup definition	
Top Flange	$(0°, 90°, 90°, 0°)$
Middle Flange	$(0°, 90°, 90°, 0°)$
Bottom Flange	$(0°, 90°, 90°, 0°)$
Right Web	$(0°, 90°, 90°, 0°)$
Left Web	$(0°, -90°, -90°, 0°)$

At a load level of $80kN$ a visual buckle initiates in the bottom flange and enhances with additional loading and a buckling pattern propagates in the bottom flange in the length direction of the box-profile. The initiation of buckling in the bottom flange results in a stiffness decrease for the structure which immediately may be observed by the change in slope for the load-deflection curve of the initial design, see Fig. 15. The buckling initiation is as already mentioned not connected to any stability point. This has been verified by singularity checks upon the tangent stiffness matrix during GNL analysis, i.e. no singular points could be found.

At buckling, the bottom flange loses its stiffness and thereby its load carrying capability and load redistribution occurs from the bottom flange to the other structural parts in the box-profile. The load carried by the bottom flange is mainly redistributed to the webs and the middle flange. The middle flange is prior to buckling almost unloaded since it lies in the neutral plane. After buckling the position of the neutral plane is shifted so it lies between the top and middle flange, i.e. the middle flange becomes compression loaded. The load redistribution that occurs in connection with the initiation of buckling in the bottom flange is well captured by the nonlinearity factor, $\varepsilon_{\mathrm{GNL}}$, which is plotted in Fig. 14 for the four fiber layers at the buckling load of $80kN$ for the initial design.

The nonlinearity factor, $\varepsilon_{\mathrm{GNL}}$, is largest for the elements in the middle flange since those elements initially are almost unloaded, thus a large change occurs in the principal strain relative to the load factor. Also the elements in the rear end of the bottom flange have nonlinearity factors differently from 1 since the bottom flange buckles and load redistribution occurs whereby the compressive principal strain relative to the load factor is reduced.

The optimization formulations stated in Table 8 are benchmarked upon the box-profile in the attempt to maximize the
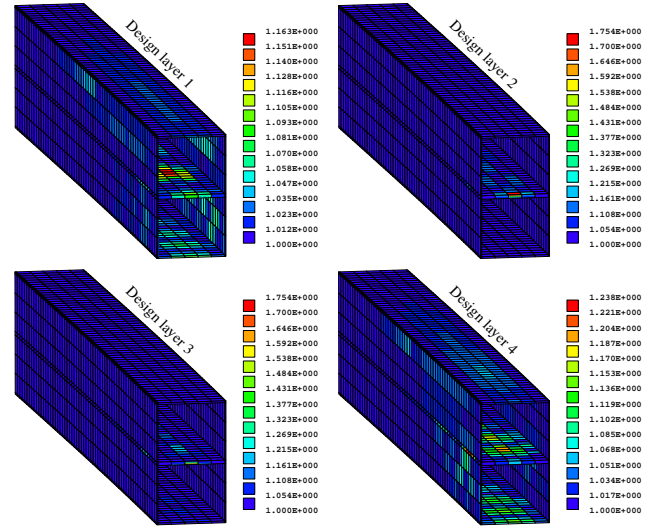
Fig. 14 Plots of the nonlinearity factor, $\varepsilon_{\mathrm{GNL}}$, for all design layers at the buckling load of the initial laminate design. Note that the box-profile is seen from the rear end.

buckling load. Since the nonlinearity factor is largest for the elements in the middle flange that are far away from the structural part that buckles, i.e. the bottom flange, it is attempted both to minimize the maximum nonlinearity factor for all elements in the model and to minimize the maximum nonlinearity factor for only the elements in the bottom flange. The optimization that operates on all elements in the model is referred to as Min Max Global $\varepsilon_{\mathrm{GNL}}$ whereas the optimization that only operates on the elements in the bottom flange is referred to as Min Max Local $\varepsilon_{\mathrm{GNL}}$. The stop criterion, $\varepsilon_{\mathrm{GNL}}$, in the GNL analysis is for local detection set to $\varepsilon_{\mathrm{GNL}} = 1.5$ and for global detection set to $\varepsilon_{\mathrm{GNL}} = 2.9$ which both are reached after visual buckling at a load level close to the buckling load. The threshold values for the nonlinearity factor used in GNL analyses are reached at approximately $85kN$ for the initial design which is just above the visually determined buckling load of $80kN$.

Although no stability point exists for the box-profile an optimization that maximizes the minimum linear buckling load is attempted. This is done since the fundamental linear buckling mode is very similar to the GNL post buckling deformation shape, see Fig. 13.

Table 8 Optimization formulations applied in the buckling optimization of the box-profile.

#	Objective function	Analysis method	Stop criterion
1.	Max Min Linear Buckling	Linear	-
2.	Min Linear Compliance	Linear	-
3.	Min Compliance	GNL	Local ε_{GNL}
4.	Min Max Global ε_{GNL}	GNL	Global ε_{GNL}
5.	Min Max Local ε_{GNL}	GNL	Local ε_{GNL}

Equilibrium curves of the optimized designs obtained by the optimization formulations stated in Table 8 are collectively shown in Fig. 15.
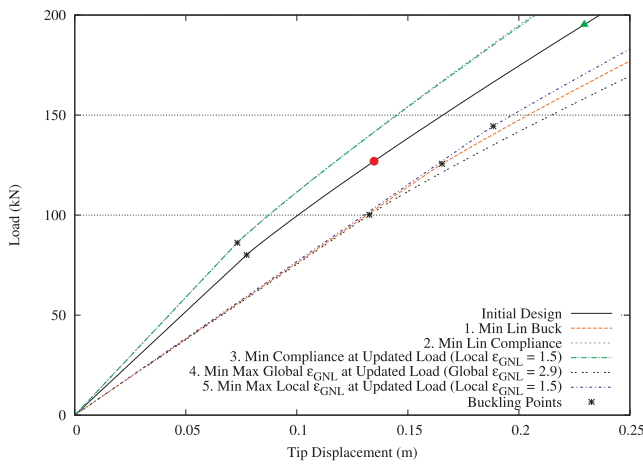
Fig. 15 Load-deflection curves of the initial laminate composite design and of the optimized designs obtained by the benchmarked optimization formulations for the box-profile.

Both optimization formulations based on minimum compliance, i.e. linear and GNL, yield almost the same equilibrium curve and only little improvement in the buckling load may be observed. The buckling load is increased by 5% and 8% by the design based on minimum linear compliance and minimum GNL compliance, respectively. As expected, the overall stiffness of the structure is increased by the optimizations based on minimum compliance.

Considering the design obtained by the maximum linear buckling load a buckling load improvement of 57% is achieved. Thus an optimization formulation based on global stability as the case for optimization formulation number two, see Table 8, is able to increase the buckling load even when no global stability point is present.

The buckling load improvement by optimization formulation number four and five is 25% and 80%, respectively. Thus optimization formulation five that operates directly upon the elements in the structural part where the buckle initiates gives a much better buckling load improvement than the optimization formulation that operates on the maximum nonlinearity factor of all elements within the model. Although

the nonlinearity factors, ε_{GNL}, for all elements are highly affected by buckling initiation in the bottom flange, not all local criterion functions are capable of representing this relation. For the elements in the structural area of instability there is a better correspondance between the local criterion functions based on the nonlinearity factor and the buckling initiation. This statement is also emphazised by the fact that the global level of ε_{GNL} is lower at the buckling point for the local ε_{GNL} optimized design than for the buckling point for the global ε_{GNL} optimized design.

8 Conclusions

In this work a range of different criterion functions for the maximum buckling resistance of laminated composite structures is benchmarked upon different numerical examples having different buckling behaviour. The majority of the criterion functions applied in the benchmark study is from literature and concerns both local and global criterion functions based on either linear or geometrically nonlinear analysis. A new local criteria function in terms of an element quantity is presented and is formulated such it gives a measure for local nonlinear effects upon loading and referred to as the element nonlinearity factor. The maximum buckling load is obtained by gradient based optimization and the design sensitivities for all criteria are determined semi-analytically by either the direct differentiation method or by the adjoint approach.

In the benchmark study buckling with stability point of the limit point type and buckling without stability point are concerned. The latter type may in principle not be classified as buckling since loss of stability does not take place. Though, the term buckling is in many cases used to describe e.g. behaviour of imperfect structures with initially stable bifurcation a.k.a. stable post buckling, structures developing visual local buckling or wrinkles upon loading without bifurcation or limiting behaviour, and structures with geometrically highly nonlinear behaviour with considerably geometry changes that act in the same manner as imperfections.

From the benchmark study it is found that different criterion functions should be applied depending on the type of buckling in order to obtain the best buckling load improvement and thereby the best performing structural design. In general do optimization formulations including non-

13

linear prebuckling effects by geometrically nonlinear analysis give better results than those based on linear analysis.

For structures exhibiting a limit point type buckling the criterion based on the nonlinear buckling load is favoured. This criterion works directly upon the limit point load and the method includes accurate nonlinear path tracing analysis where the buckling load is estimated at a precritical point on the deformed configuration. The estimation point is always chosen close to the real buckling point for a precise estimate of the nonlinear buckling load and the nonlinear buckling load design sensitivities. Compared to the other criterion functions benchmarked, the nonlinear buckling load criterion is far superior in the case of limit point buckling.

For cases where buckling alike patterns develop with the absence of a stability point, i.e. buckling without a stability point, the local criteria, referred to as the element nonlinearity factor, yield the best buckling load improvement. The element measure is able to detect local nonlinear effects upon loading, in particular load redistribution which often takes place with local buckling pattern development. In the numerical studies it was found that the element nonlinearity factor in some cases may have values in parts of the structure that are larger than where the buckling pattern propagates. For such cases it is better to focus the optimization on the part of the structure where the buckling pattern initiates in order to obtain the best buckling load improvement and suppression of the buckling pattern.

References

Abrate S (1994) Optimal design of laminated plates and shells. Compos Struct 29:269–286

Almroth BO, Brogan FA (1972) Bifurcation buckling as an approximation of the collapse load for general shells. AIAA J 10(4):463–467

Bendsøe MP, Sigmund O (2003) Topology optimization - theory, methods and applications, 2nd edn. Springer Verlag Berlin Heidelberg New York, ISBN: 3-540-42992-1

Bendsøe MP, Olhoff N, Taylor J (1983) A variational formulation for multicriteria structural optimization. J Struct Mech 11:523–544

Borri C, Hufendiek HW (1985) Geometrically nonlinear behaviour of space beam structures. J Struct Mech 13:1–26

Brendel B, Ramm E (1980) Linear and nonlinear stability analysis of cylindrical shells. Compt Struct 12:549–558

Brush DO, Almroth BO (1975) Buckling of bars, plates, and shells. McGraw-Hill Kogakusha, ISBN: 07-085028-3

Bushnell D (1985) Computerized buckling analysis of shells. Martinus Nijhoff Publishers, ISBN: 90-247-3099-6

Courant R, Hilbert D (1953) Methods of mathematical physics, vol 1. New York : Interscience Publishers

Crisfield MA (1981) A fast incremental/iterative solution procedure that handles "snap-through". Compt Struct 13:55–62

Dvorkin EN, Bathe KJ (1984) A continuum mechanics based four-node shell element for general non-linear analysis. Eng Comput 1:77–88

Foldager JP, Hansen JS, Olhoff N (2001) Optimization of the buckling load for composite structure taking thermal effects into account. Struct Multidiscip Optim 21:14–31

Harnau M, Schweizerhof K (2002) About linear and quadratic "solid-shell" elements at large deformations. Compt Struct 80(9-10):805–817

Hinton E (ed) (1992) NAFEMS Introduction to Nonlinear Finite Element Analysis. Bell and Bain Ltd, Glasgow, ISBN 1-874376-00-X

Hu HT, Wang SS (1992) Optimization for buckling resistance of fiber-composite laminate shells with and without cutouts. Compos Struct 22(2):3–13

Hu HT, Yang JS (2007) Buckling optimization of laminated cylindrical panels subjected to axial compressive load. Compos Struct 81:374–385

Hyer MW, Lee HH (1991) The use of curvilinear fiber format to improve buckling resistance of composite plates with central circular holes. Compos Struct 18(5/6):239–261

Johansen L, Lund E, Kleist J (2009) Failure optimization of geometrically linear/nonlinear laminated composite structures using a two-step hierarchical model adaptivity. Compt Methods Appl Mech Engrg 198(30-32):2421–2438

Jones RM (2006) Buckling of bars, plates, and shells. Bull Ridge Publishing, ISBN: 0-9787223-0-2

Klinkel S, Gruttmann F, Wagner W (1999) A continuum based three-dimensional shell element for laminated structures. Compt Struct 71 (1):43–62

Lee SJ, Hinton E (2000) Dangers inherited in shells optimized with linear assumptions. Compt Struct 78:473–486

Lin CC, Yu AJ (1991) Optimum weight design of composite laminated plates. Compt Struct 38(5/6):581–587

Lindgaard E, Lund E (2010a) Nonlinear buckling optimization of composite structures. Compt Methods Appl Mech Engrg 199(37-40):2319–2330, DOI 10.1016/j.cma.2010.02.005

Lindgaard E, Lund E (2010b) A unified approach to nonlinear buckling optimization of composite structures. Submitted

Lindgaard E, Lund E, Rasmussen K (2010) Nonlinear buckling optimization of composite structures considering "worst" shape imperfections. Int J Solids Struct 47:3186–3202, DOI 10.1016/j.ijsolstr.2010.07.020

Lund E (2009) Buckling topology optimization of laminated multi-material composite shell structures. Compos Struct 91:158–167

Lund E, Stegmann J (2005) On structural optimization of composite shell structures using a discrete constitutive parametrization. Wind Energy 8:109–124, DOI 10.1002/we.132

Mateus HC, Soares CMM, Soares CAM (1997) Buckling sensitivity analysis and optimal design of thin laminated structures. Compt Struct 64(1-4):461–472

Moita JS, Barbosa JI, Soares CMM, Soares CAM (2000) Sensitivity analysis and optimal design of geometrically non-linear laminated plates and shells. Compt Struct 76:407–420

Noguchi H, Hisada T (1993) Sensitivity analysis in post-buckling problems of shell structures. Compt Struct 47(4/5):699–710

Olhoff N (1989) Multicriterion structural optimization via bound formulation and mathematical programming. Struct Optim 1:11–17

Overgaard LCT, Lund E (2005) Structural design sensitivity analysis and optimization of vestas V52 wind turbine blade. In: Proc. 6th World Congress on Structural and Multidisciplinary Optimization

Overgaard LCT, Lund E, Thomsen OT (2010) Structural collapse of a wind turbine blade. Part A: Static test and equivalent single layered models. Composites Part A 41(2):257–270, DOI 10.1016/j.compositesa.2009.10.011

Singer J, Arbocz J, Weller T (1998) Buckling experiments: Experimental methods in buckling of thin-walled structures, vol 1. John Wiley & Sons, ISBN: 0-471-95661-9

Svanberg K (1987) Method of moving asymptotes - a new method for structural optimization. Int J Numer Methods Eng 24:359–373

Taylor JE, Bendsøe MP (1984) An interpretation of min-max structural design problems including a method for relaxing constraints. Int J Solids Struct 20(4):301–314

Thompson JMT, Hunt GW (1973) A general theory of elastic stability. John Wiley & Sons, ISBN: 0-471-85991-5

Topal U (2009) Multiobjective optimization of laminated composite cylindrical shells for maximum frequency and buckling load. Mater Des 30:2584–2594

Topal U, Uzman Ü (2008) Maximization of buckling load of laminated composite plates with central circular holes using mfd method. Struct Multidiscip Optim 35:131–139

Walker M (2001) Multiobjective design of laminated plates for maximum stability using the finite element method. Compos Struct 54:389–393

Walker M, Adali S, Verijenko V (1996) Optimization of symmetric laminates for maximum buckling load including the effects of bending-twisting coupling. Compt Struct 58(2):313–319

Wilson EL, Itoh T (1983) An eigensolution strategy for large systems. Compt Struct 16:259–265

Wittrick WH (1962) Rates of change of eigenvalues, with reference to buckling and vibration problems. J Roy Aeronaut Soc 66:590–591

A Design sensitivity analysis

A.1 Linear displacement sensitivity

The displacement sensitivities $\frac{d\mathbf{D}}{da_i}$ are computed by direct differentiation of the static equilibrium equation, see (1), w.r.t. a design variable $a_i, i = 1, \ldots, I$.

$$\mathbf{K_0}\frac{d\mathbf{D}}{da_i} = -\frac{d\mathbf{K_0}}{da_i}\mathbf{D} + \frac{d\mathbf{R}}{da_i}, \quad i = 1, \ldots, I \tag{15}$$

The displacement sensitivity $\frac{d\mathbf{D}}{da_i}$ can be evaluated by backsubstitution of the factored global initial stiffness matrix in (15). The initial stiffness matrix has already been factored when solving the static problem in (1) and can here be reused, whereby only the new terms on the right hand side of (15), called the pseudo load vector, need to be calculated. Note that the force vector derivative, $\frac{d\mathbf{R}}{da_i}$, is zero for design independent loads as in the case for CFAO. The global initial stiffness matrix derivatives $\frac{d\mathbf{K_0}}{da_i}$ are determined semi-analytically at the element level by central difference approximations and assembled to global matrix derivatives.

$$\frac{d\mathbf{k_0}}{da_i} \approx \frac{\mathbf{k_0}(a_i + \Delta a_i) - \mathbf{k_0}(a_i - \Delta a_i)}{2\Delta a_i} \tag{16}$$

$$\frac{d\mathbf{K_0}}{da_i} = \sum_{n=1}^{N_e^{as}}\frac{d\mathbf{k_0}}{da_i}, \quad i = 1, \ldots, I \tag{17}$$

$\mathbf{k_0}$ is the element initial stiffness matrix, Δa_i is the design perturbation, and N_e^{as} is the number of elements in the finite element model associated to the design variable a_i.

A.2 Nonlinear displacement sensitivity

The nonlinear displacement sensitivities are computed by considering the residual or force unbalance equation at a converged load step n,

$$\mathbf{Q}^n(\mathbf{D}^n(\mathbf{a}), \mathbf{a}) = \mathbf{F}^n - \mathbf{R}^n = \mathbf{0} \tag{18}$$

where $\mathbf{Q}^n(\mathbf{D}^n(\mathbf{a}), \mathbf{a})$ is the so-called residual or force unbalance, $\mathbf{F}^n$ is the global internal force vector, and $\mathbf{R}^n$ is the global applied load

vector. Taking the total derivative of this equilibrium equation with respect to any of the design variables $a_i, i = 1, \ldots, I$, we obtain

$$\frac{d\mathbf{Q}^n}{da_i} = \frac{\partial\mathbf{Q}^n}{\partial a_i} + \frac{\partial\mathbf{Q}^n}{\partial\mathbf{D}^n}\frac{d\mathbf{D}^n}{da_i} = \mathbf{0} \tag{19}$$

where

$$\frac{\partial\mathbf{Q}^n}{\partial\mathbf{D}^n} = \frac{\partial\mathbf{F}^n}{\partial\mathbf{D}^n} - \frac{\partial\mathbf{R}^n}{\partial\mathbf{D}^n} \tag{20}$$

and

$$\frac{\partial\mathbf{Q}^n}{\partial a_i} = \frac{\partial\mathbf{F}^n}{\partial a_i} - \frac{\partial\mathbf{R}^n}{\partial a_i} \tag{21}$$

We note that (20) reduces to the tangent stiffness matrix. Since it is assumed that the current load is independent of deformation, $\frac{\partial\mathbf{R}^n}{\partial\mathbf{D}^n} = \mathbf{0}$, we obtain

$$\frac{\partial\mathbf{F}^n}{\partial\mathbf{D}^n} = \mathbf{K}_{\mathbf{T}}^n \tag{22}$$

By inserting the tangent stiffness and (21) into (19), we obtain the displacement sensitivities $\frac{d\mathbf{D}^n}{da_i}$ as

$$\mathbf{K}_{\mathbf{T}}^n\frac{d\mathbf{D}^n}{da_i} = \frac{\partial\mathbf{R}^n}{\partial a_i} - \frac{\partial\mathbf{F}^n}{\partial a_i} \tag{23}$$

The partial derivative of the load vector, $\frac{\partial\mathbf{R}^n}{\partial a_i}$, can explicitly be expressed by two terms by taking the partial derivative to (6)

$$\frac{\partial\mathbf{R}^n}{\partial a_i} = \gamma^n\frac{\partial\mathbf{R}}{\partial a_i} + \frac{\partial\gamma^n}{\partial a_i}\mathbf{R} \tag{24}$$

For design independent loads $\frac{\partial\mathbf{R}}{\partial a_i} = \mathbf{0}$ and for a fixed load level $\frac{\partial\gamma^n}{\partial a_i} = 0$. The pseudo load vector, i.e. the right hand side to (23), is determined at the element level by central difference approximations and assembled to global vector derivatives.

A.3 Linear compliance

The design sensitivity of linear compliance is obtained by applying the adjoint approach, see e.g. Bendsøe and Sigmund (2003); Lund and Stegmann (2005), and obtaining the sensitivity with respect to any design variable $a_i, i = 1, \ldots, I$ as

$$\frac{dC_L}{da_i} = -\mathbf{D}^{\mathrm{T}}\frac{d\mathbf{K_0}}{da_i}\mathbf{D} \tag{25}$$

The global initial stiffness matrix derivatives $\frac{d\mathbf{K_0}}{da_i}$ are determined semi-analytically at the element level by central difference approximations and assembled to global matrix derivatives as in (16) and (17).

A.4 Nonlinear end compliance

The design sensitivity of nonlinear end compliance at a converged load step n with respect to any design variable, $a_i, i = 1, \ldots, I$, is obtained by the adjoint approach, see e.g. Bendsøe and Sigmund (2003)

$$\frac{dC_{GNL}}{da_i} = \boldsymbol{\lambda}^{\mathrm{T}}\frac{\partial\mathbf{Q}^n}{\partial a_i} = \boldsymbol{\lambda}^{\mathrm{T}}\left(\frac{\partial\mathbf{F}^n}{\partial a_i} - \frac{\partial\mathbf{R}^n}{\partial a_i}\right) \tag{26}$$

Assuming the end load fixed and independent of design changes we have that $\frac{\partial\mathbf{R}^n}{\partial a_i} = \mathbf{0}$. The adjoint vector $\boldsymbol{\lambda}$, which is not to be confused with the eigenvector, is obtained as the solution to the adjoint equation

$$\mathbf{K}_{\mathbf{T}}^n\boldsymbol{\lambda} = -\mathbf{R}^n \tag{27}$$

The partial derivatives in the right hand side of (26) are determined at the element level by central difference approximations and assembled to global vector derivatives.

A.5 Nonlinear first principal element strain

The design sensitivities of the first principal element strain, $\frac{d\varepsilon_1}{da_i}$, are determined semi-analytically by forward differences at the element level.

$$\frac{d\varepsilon_1}{da_i} \approx \frac{\varepsilon_1(\mathbf{D}^n + \Delta\mathbf{D}^n) - \varepsilon_1(\mathbf{D}^n)}{\Delta a_i} \tag{28}$$

The displacement field is perturbed via the calculated displacement sensitivities in (23) such that $\Delta\mathbf{D}^n \approx \frac{d\mathbf{D}^n}{da_i}\Delta a_i$.

A.6 Element nonlinearity factor

The design sensitivities of the element nonlinearity factor, $\varepsilon_{\mathrm{GNL}}$, are determined semi-analytically by forward differences at the element level.

$$\frac{d\varepsilon_{\mathrm{GNL}}}{da_i} \approx \frac{\varepsilon_{\mathrm{GNL}}(\mathbf{D}^1 + \Delta\mathbf{D}^1, \mathbf{D}^n + \Delta\mathbf{D}^n) - \varepsilon_{\mathrm{GNL}}(\mathbf{D}^1, \mathbf{D}^n)}{\Delta a_i} \tag{29}$$

It is assumed that the initial load level and the final load level are fixed whereby the perturbed element nonlinearity factor is determined by

$$\varepsilon_{\mathrm{GNL}}(\mathbf{D}^1 + \Delta\mathbf{D}^1, \mathbf{D}^n + \Delta\mathbf{D}^n) = \tag{30}$$
$$1 + \left| \frac{\varepsilon_1^n(\mathbf{D}^n + \Delta\mathbf{D}^n)/\gamma^n - \varepsilon_1^1(\mathbf{D}^1 + \Delta\mathbf{D}^1)/\gamma^1}{\varepsilon_1^1(\mathbf{D}^1 + \Delta\mathbf{D}^1)/\gamma^1} \right|$$

Since the element nonlinearity factor is determined by information at two equilibrium points, i.e. the initial load step and the final step n, the displacement sensitivities have to be calculated at both load steps by (23). The perturbation of the displacement fields at both equilibrium points may then be evaluated by $\Delta\mathbf{D}^n \approx \frac{d\mathbf{D}^n}{da_i}\Delta a_i$ and $\Delta\mathbf{D}^1 \approx \frac{d\mathbf{D}^1}{da_i}\Delta a_i$, respectively.

A.7 Linear buckling

The linear buckling load factor sensitivities may be determined by

$$\frac{d\lambda_j}{da_i} = \boldsymbol{\phi}_j^T \left(\frac{d\mathbf{K_0}}{da_i} + \lambda_j \frac{d\mathbf{K_\sigma}}{da_i} \right) \boldsymbol{\phi}_j \tag{31}$$

where the eigenvalue problem in (2) has been differentiated with respect to any design variable, $a_i, i = 1, \ldots, I$, assuming that λ_j is simple, see e.g. Courant and Hilbert (1953); Wittrick (1962). The global matrix derivatives of $\mathbf{K_0}$ and $\mathbf{K_\sigma}$ are determined semi-analytically at the element level by central difference approximations and assembled to global matrix derivatives, see (16) and (17). The stress stiffness matrix is an implicit function of the displacement field, i.e. $\mathbf{K_\sigma}(\mathbf{D}(\mathbf{a}), \mathbf{a})$, thus both displacement field and design variables need to be perturbed in the element central difference approximation. The displacement field is perturbed via the calculated displacement sensitivities in (23) such that $\Delta\mathbf{D}^n \approx \frac{d\mathbf{D}^n}{da_i}\Delta a_i$.

A.8 Nonlinear buckling

The nonlinear buckling load factor sensitivities at load step n are determined by

$$\frac{d\lambda_j}{da_i} = \boldsymbol{\phi}_j^T \left(\frac{d\mathbf{K_0}}{da_i} + \frac{d\mathbf{K_L^n}}{da_i} + \lambda_j \frac{d\mathbf{K_\sigma^n}}{da_i} \right) \boldsymbol{\phi}_j \tag{32}$$

and

$$\frac{d\gamma_j^c}{da_i} = \frac{d\lambda_j}{da_i} \gamma^n \tag{33}$$

where the eigenvalue problem in (11) has been differentiated with respect to any design variable, $a_i, i = 1, \ldots, I$, assuming that λ_j is simple, see Lindgaard and Lund (2010a). It is assumed that the final load level is fixed and that the nonlinear buckling load has been determined at load step n by evaluation of (10) and (11). The global matrix derivatives of $\mathbf{K_0}$, $\mathbf{K_L^n}$, and $\mathbf{K_\sigma^n}$ are determined in the same manner as for the linear buckling load sensitivities, i.e. semi-analytical central difference approximations at the element level and assembly to global matrix derivatives.